Contents list available at IJRED website

International Journal of Renewable Energy Development

Journal homepage: https://ijred.undip.ac.id

Research Article

Energy Management Strategy Based on Marine Predators Algorithm for Grid-Connected Microgrid

Amel Kheiter*, Slimane Souag, Abdellah Chaouch, Abdelkader Boukortt, Benaissa Bekkouche, Mohammed Guezgouz

Faculty of Science and Technology, Electrical Engineering Department, ECP3M Laboratory, Abdelhamid Ibn Badis University of Mostaganem, 27000 Mostaganem, Algeria

Abstract. This work aims to optimize the economic dispatch problem of a microgrid system in order to cover the load of a commercial building in Algeria. The analyzed microgrid system is connected to the power grid and composed of photovoltaic panels (PV), wind turbine, battery energy storage system (BESS) and diesel generator. To ensure energy balance and the flow of energy, we have implemented an energy management strategy based on Marine Predator Algorithm (MPA) and Multilayer Perceptron Neural Network (MLPNN), which guarantee an optimal economic operation of the system. First, using historical meteorological data, the power generation is forecasted a day-ahead using MLPNN, which allows the optimization of the microgrid operation. Second, the proposed strategy has been studied under three different microgrid configurations. Eventually, the performances of MPA are compared against well-known algorithms. The results indicate that the integration of the PV-BESS microgrid system significantly reduces the daily operating cost up to 34.5%. Due to the availability of wind resources in the studied area, the addition of a wind turbine to the microgrid minimizes the operating cost by 43.96% compared to the operating cost of the power grid. In the case of selling excess energy to the main power grid, the operating cost could be decreased as much as 49.33%.

Keywords: Hybrid system; Photovoltaic; Wind system; Energy management strategy; Artificial intelligence; Deep Learning algorithms

Received: 20th Nov 2021; Revised: 14th April 2022; Accepted: 26th April 2022; Available online: 8th May 2022

1. Introduction

Renewable energy sources are perceived as the best way to reduce successfully greenhouse gas (GHG) emissions from the electricity sector (Kilickaplan, 2017). Subsequently, the world is witnessing a transition to a sustainable energy future, which leads to economic prosperity and limited GHG (Hajer & Pelzer, 2018). During 2020, according to the IRENA report (Adrian Whiteman), more than 260 GW of renewable energy capacity has been installed worldwide, 91% of which is wind and solar energy. On one hand, this statistic indicates the importance of these viable sources of energy. On the other hand, Algeria is one of the countries endowed with high solar potential and climatic diversity (Guezgouz *et al*, 2021). Therefore, the government has taken a number of actions to facilitate the investment in these sustainable resources (Stambouli *et al*, 2012). Recently, several projects have seen the light in the South of Algeria according to the national program of development of renewable energies (2015-2030) (Abhishek *et al* 2012; Sonelgaz. Available online: http://www.sonelgaz.dz/ [accessed on 2020).

Besides the environmental benefits and abundance availability of renewable energies, their intermittency is a major drawback that prevents the optimal use of these energies (Clarke *et al* 2013). The employment of a microgrid system is one of the best solutions to this problem since the integration of a number of resources could partially mitigate renewables variability. Moreover, the power flow should be optimized in order to ensure the optimal operation of the system (Suberu *et al*, 2014). Therefore, it is necessary to conceive a smart energy management strategy (EMS) to maintain the balance between production and consumption at each moment. In addition, EMS should guarantee the continuity of power supply while minimizing operating costs and the purchasing power from the power grid (Naeem & Hassan, 2020). In the next sub-section, we provide a general overview on microgrid studies and energy management strategies.

Microgrid systems have gained increased interest among researchers aiming for reducing renewable energy costs to facilitate their integration and deployment (Moran, 2016). Recently, Al-Zoubi *et al* (2021) conducted a feasibility study for covering a hotel load using a grid-connected PV system. The authors have used PVsyst and PVgis software in order to design and analyse the economic performances of the system. It has been validated that a grid-connected photovoltaic system is a technically and economically viable for the electrification of residential hotel applications (Al-Zoubi *et al* 2021). Karthik *et al*

* Corresponding author
Email: amel.kheiter.etu@univ-mosta.dz (A. Kheiter)

https://doi.org/10.14710/ijred.2022.42797
ISSN: 2252-4940/© 2022.The Author(s). Published by CBIORE

(2021) proposed a multi-objective approach based on the Levy flight algorithm in order to optimize the power flow of a wind-solar system coupled with a conventional thermal power source. Their results indicated the superiority of the proposed method in terms of exploration of the search space and convergence towards an optimal solution (Karthik *et al*, 2021). Brenna *et al*, simulated PV system and energy storage technologies considering electrical vehicles in order to explore their impact on the centralized power system, they deduced that the future adoption of rooftop photovoltaic panels and the impact on centralized generation is incredibly higher than the adoption of energy storage systems (Brenna *et al*, 2020). Neto *et al*, proposed a reliable energy management strategy based on the virtual inertia concept with the aim of simplifying the communication link between the grid and the energy storage system of a DC microgrid (Neto *et al*., 2020). Dong *et al* (2020), optimized the EMS of a microgrid system consisting of PV, wind, microturbine and battery systems, based on a multi-agent system and hierarchic game theory algorithm. Their findings showed the cost-benefits of the proposed method (Dong *et al*, 2020). For the same on-grid microgrid components, Nimma *et al*. (2018) optimized the sizing and EMS of the system using Grey Wolf Optimizer. Their outcomes confirmed the outperformance of GWO against the most well-known algorithms (Nimma *et al*., 2018). Peng *et al*, performed an optimal control of DC microgrid using rigorous Lyapunov synthesis for minimizing the production cost together with the regulation of bus voltage (Peng *et al* 2021). Luu Ngoc and Tran (2015) optimized a microgrid EMS including PV-wind-BESS using a Brunch and Bound method to minimize the operating costs, CO_2 emissions and electricity purchased from the main electricity network. Brunch and Bound method achieved the optimal value the state of charge which allows minimum cash flow (Luu Ngoc & Tran, 2015). In the same vein, Iqbal *et al*, explored the performances of several meta-heuristic algorithms in solving the economic dispatch of a microgrid system covering the load of a smart house, the results of this comparative study confirm the ability of these methods in minimizing the cost of electricity (Iqbal *et al*., 2018). Tayab *et al*. investigated the day-ahead scheduling problem using particle swarm optimization (PSO) for PV-battery system. The proposed swarm intelligence-based method along with forecasting module was examined throughout MATLAB Simulink simulation (Tayab *et al* 2018). Using the same Algorithm, Wang *et al*, optimized the EMG for microgrid system in IEEE-9 buses system (Wang *et al* 2017). Arcos-Aviles *et al* (2018) scrutinized experimentally the performances of Fuzzy logic-based EMS for a residential microgrid system. The proposed controller minimized the grid fluctuations while keeping the state of charge (SOC) of the battery storage within a secure range (Arcos-Aviles *et al*, 2018). Vergara *et al*. introduced a real-time EMS based on a no-dominated sorting Genetic algorithm, where the crossover and mutation parameters were adapted in order to achieve higher performances (Vergara *et al* 2015). Ahmad Eid *et al*. (2021) improved marine predator algorithm (MPA) to control the active and reactive power injected into two standard distribution test systems and to minimize system losses. The simulation results showed that MPA is characterized by better convergence towards optimal solutions. Moreover, MPA outperforms its counterparts in terms of ensuring the reliability for the tested system (Eid *et al* 2021). Sobhy *et al*. (2021) optimized a design of a modern proportional-integral-derivative (PID) controllers using MPA. Again, optimization comparison of MPA against other competing methods was conducted. In addition, the results highlighted the role of energy storage units in enhancing the time-domain transient responses. (Sobhy *et al* 2021). Shaheen *et al* (2020) used an improved marine predator algorithm and particle swarm algorithm (IMPAPSO) to solve the Optimal Power Distribution Problem (ORPD) for standard networks, IEEE 30 buses and IEEE 57 buses. It was reported that the improved algorithm is characterized by its rapid convergence when compared with its counterparts. Furthermore, there was a great improvement in the power grid operation after minimizing active power losses and voltage deviation (Shaheen *et al,* 2020).

In summary, prior studies have common features such as system components and artificial intelligence-based optimization. Commonly, the studied microgrid is composed of PV panels, wind turbines and a storage energy system (BESS). Most often, a diesel generator supports these components of the microgrid system or it is connected to the power grid. Generally, the authors applied algorithms based on swarm intelligence in order to optimize EMS for microgrid systems. The objective functions are usually formulated to obtain the best management of the energy flow, while minimizing the daily operating costs of the microgrid, maximizing the use of renewable energies and reducing dependence on the main grid.

In order to facilitate the integration of renewable energy sources, this work proposed a smart energy management strategy to optimize the performance of a grid-connected microgrid system. The latter is composed of two renewable energy resources (photovoltaic panels and wind turbines); a diesel generator and BESS are also considered as backup systems. In order to estimate renewable generation, we have used MLPNN algorithm to forecast temperature, solar irradiance and wind speed. Then, the forecasted weather data are used as inputs in the mathematical models of PV array and wind turbine to estimate their power generation. After that, the energy dispatch is optimized by the MPA which is a new meta-heuristic inspired from the strategy of foraging for food in oceanic predators. MPA is chosen to solve the economic dispatch problem of the microgrid, while minimizing its daily operating cost. Moreover, the performance of MPA is compared against well-known meta-heuristic algorithms, namely, Particle swarm optimization (PSO), Genetic Algorithm (GA) and Gravitational Search Algorithm (GSA).

2. Study Framework

Algeria is a large country and is characterized by different geographical topology and climate conditions. It has an abundant renewable energy potential spatially in terms of solar radiation and wind potential (Dahmoun *et al*., 2021; Guezgouz *et al* 2019). Therefore, the establishment of microgrid systems to meet the electricity demand at the lowest cost is an attractive option for reducing reliance of the electricity sector on conventional-powered stations (Tang *et al* 2014; Ton & Smith, 2012).

This work is a hypothetical study carried out on a commercial building with a typical load in Algeria supplied by the main power grid and a backup diesel generator as shown in Figure 1. This study proposed the integration microgrid system to cover partially of the electrical demand of the commercial building.

The architecture of the proposed microgrid system is depicted in Figure 2. An intelligent energy management system is implemented so the energy balance will be ensured and the daily operating cost will be minimized.

3. Methodology

The main contribution of this study is proposing an intelligent energy management strategy based on both Deep Learning (MLPNN) and artificial intelligence (MPA) algorithms. The proposed method allows a cost-effective energy dispatch of the microgrid, while it maintains the continuity of power supply. In this context, we explore three different scenarios where we have included renewable energies as distributed sources to cover the electrical demand of a commercial building in Algeria. The first scenario is characterized by the integration of the PV system and BESS to the existing main grid and the backup diesel generator in order to cover the load demand. In the second scenario, we have integrated another key role renewable energy source, the wind system in addition to the previous generators. Similarly, the third scenario could sell excess energy from renewables energies to the power grid after achieving demand coverage, which minimizes further the daily microgrid operating costs. The following sub-section describes the modeling of the considered systems: PV, wind turbine and the battery storage system.

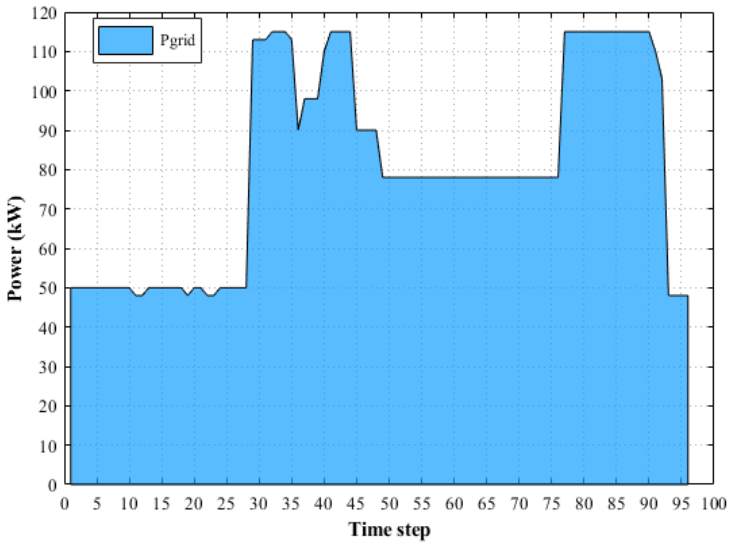

Fig 1. The commercial load studied powered from the national power grid.

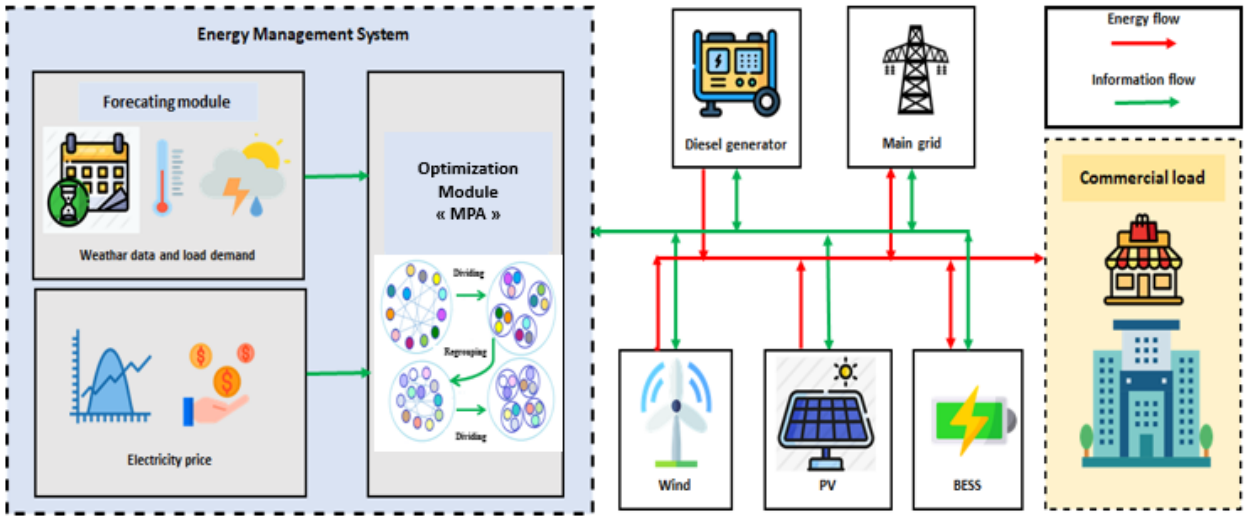

Fig 1. Architecture of the proposed Microgrid system.

3.1. Modeling of the photovoltaic system

The mathematical model proposed by National Renewable Energy Laboratory (NREL) presented in equations (1) is used to calculate the output power of the photovoltaic system (Jurasz & Ciapała, 2017) .

$$P_{PV\_out}(t,r) = P_{Pv} \times \frac{r}{r_{ref}} \times [1 + k_t(t_c - t_{ref})] \times f_{Pv} \quad (1)$$

Where: P_{Pv}: the nominal power (kW) of the PV array,r:solar radiation (kW/m²) received by an inclined plane.r_{ref}: solar radiation under reference conditions (STD), (1000 W/m²), k_t: temperature coefficient and its value equal to -3.7×10^{-3} (1/°C), f_{Pv}: factor of losses due to dust, shade and losses by the Joule effect, t_{ref}: temperature under STD conditions (25°C), t_c:cell temperature (°C), expressed by the following equation (Kaabeche *et al*, 2017):

$$t_c = t_{em} + (\frac{NOCT-20}{800}) \times r \quad (2)$$

t_{em}: ambient temperature (°C), $NOCT$: nominal operating temperature of the PV module (°C).

3.2. Modeling of the wind power system

Each wind turbine (WT) is characterized by its power curve which facilitates the evaluation of the power that can be produced by the WT. Enercon E-18/80 wind turbine is considered and modeled based on the preceding concept. The output power of WT is calculated using the following equation (3) (Canales *et al*, 2021):

$$P_{WT} = \begin{cases} 0 & V < V_d; V > V_a \\ P_r & V_d < V < V_r \\ P_n & V_r < V < V_a \end{cases} \quad (3)$$

Where: P_{WT}: the output power of the wind turbine,P_r: power curve fitting (Figure 3), P_n: the nominal power of the wind turbine,V_d, V_a, V_r: are the cut-off wind speed, the cut-out wind speed and the nominal wind speed respectively, where V_d= 2.50m/s , V_a= 25.0m/s, V_r=12.0m/s.

Power curve of Enercon E-18/80 is shown in the Figure 3.

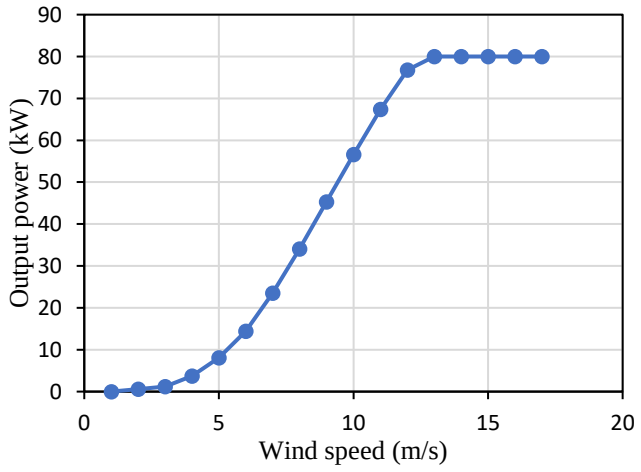

Fig 2. Power curve of Enercon E-18/80 kW wind turbine.

3.3. Modeling of the battery energy storage system

The battery energy storage system is modeled based on the charging and discharging of its stored energy which is expressed by the difference between the energy produced from the renewable generators (PV and wind turbine) and the electricity demand. Upon charging of the BESS in the case of surplus energy phase, the state of charge (SOC) of BESS is calculated by the following equation (Canales *et al.*, 2021; Guezgouz *et al.*, 2019):

$$SOC(t) = SOC(t-1) + \frac{[(E_{prod}(t) - E_{load}(t)/\eta_{inv}) \times \eta_{bat\_ch}] \times 100}{E_{BESS,max}} \quad (4)$$

During the discharge phase, the SOC of BESS can be described as follows (Canales et al., 2021; Guezgouz, Jurasz, Bekkouche, et al., 2019):

$$SOC(t) = SOC(t-1) - \frac{[(E_{load}(t)/\eta_{inv} - E_{prod}(t)) / \eta_{bat\_dis}] \times 100}{E_{BESS,max}} \quad (5)$$

Where: $SOC(t)$ and $SOC(t-1)$ are the state of BESS at time step t and t-1 respectively. $E_{load}(t)$ is the energy of the charge at time t, $E_{prod}(t)$ is the total energy produced by the generators such as the photovoltaic system, the wind turbine, the diesel generator and/or the energy purchased from the main grid. η_{inv}, η_{bat_ch}, η_{bat_dis} are the efficiency of the inverter, the charge efficiency of the BESS and the discharge efficiency, respectively. Table 1 shows the characteristics of the renewable energy technologies and the BESS specifications.

4. Proposed microgrid energy management strategy

Since the microgrid system is connected to the main grid, it is possible to sell and purchase power from it. However, the electricity price is varying according to Figure 6. Besides, photovoltaic and wind energy are intermittent and depend on weather conditions. To predict the power output of these systems, MLPNN is trained based on historical weather data. The output of this algorithm is fed to simulation model of the system, where the output power is estimated. However, it is difficult to make the optimal decision, when to purchase or sale electricity to the main grid, discharge or charge the batteries in the right time step. Therefore, MPA is proposed to optimize the operation of the microgrid system by dispatching the available power and hence reducing the daily operating costs. The flowchart presented in Figure 4 summarizes the main steps of the proposed microgrid energy management strategy using MLPNN and MPA.

4.1. Forecasting module

In order to improve the operational safety and efficient planning of the microgrid, it is necessary to forecast the output power of the PV and WT systems (Bochenek *et al.*, 2021; Theocharides *et al*, 2018). In this work, Machine Learning based method is applied to forecast the meteorological data in a day-ahead, hence, the power output of renewable energy sources will be estimated in order to be fed later to the optimization module (Liu *et al*, 2020; Nezhad *et al*, 2020).

Table 1
Characteristics of renewable energy sources and BESS.

Description	Input data
PV system	
Installed capacity	150 Kw
Rated capacity	400 W
Base material	Polycrystalline
Efficiency	95%
Lifetime	25 years
Wind turbine	
Installed capacity	80 Kw
number of WT	1
Efficiency	95%
Lifetime	15nyears
Battery Energy Storage System	
Installed capacity	90 Kw
Lifetime	10 years
Round Trip Efficiency	85%

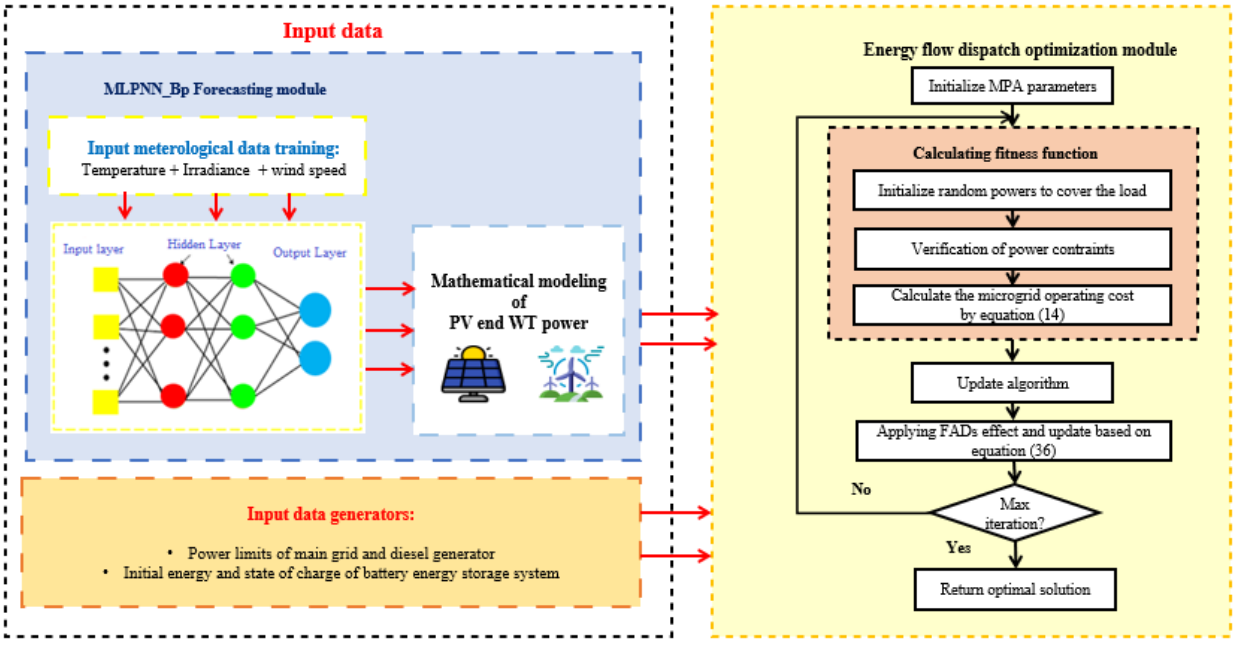

Fig 3. Flow chart of Microgrid Energy Management Strategy using MPA

The estimation of the PV and wind energy is done by the prediction of the temperature, the irradiance and the wind speed which will be used as inputs in the models of PV and WT systems explained in the previous section. In order to forecast the meteorological data in this work, we have applied MLPNN method.

4.1.1. Multilayer perceptron neural network

Multilayer perceptron neural network is introduced by Rosenblatt (Beccali *et al*, 2004), it allows the interconnection of a set of layered neurons. MLPNN is composed of three main layers, namely an input layer, one or more hidden layers and an output layer (Figure 5).

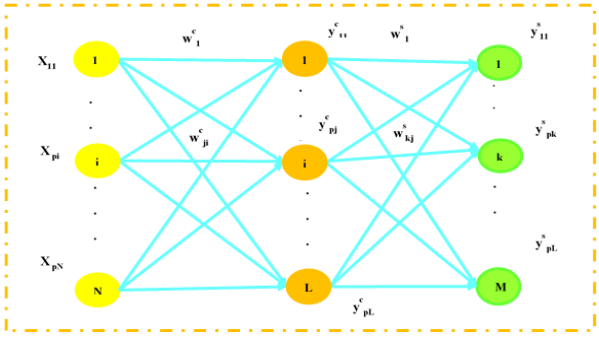

Fig 4. Architecture of a multilayer perceptron with a single hidden layer.

Where: X_{pi} the input of the i^{th} neuron of the input layer (learning input), w^c_{ji}: the weight connecting the i^{th} neuron of the input layer with the j_{th} neuron of the hidden layer, y^c_{pj}: the output of the j_{th} neuron from the hidden layer, w^s_{kj}: the weight connecting the j_{th} neuron of the hidden layer with the k_{th} of the output layer, y^s_{pk}: the output of the k_{th} neuron of the output layer.

The back-propagation method is employed in this work to train the artificial neurone network. The learning process can be organized as follows (Crow, Mar. 2015):

- Present an example from the learning set.
- Determine the exit from the network.
- Calculate the error gradients.
- Modify synaptic weights.
- Reach a stop criterion.

4.1.2. Back-propagation algorithm

The main steps of the back-propagation algorithm are summarized as follows:

i. Set an input vector.

ii. Calculate the values that connect the input neurons with that of the hidden layer according to the following equation:

$$y^c_{pj} = f(\sum_{i=1}^{N} w_{ji} \times x_{pi}) \quad (6)$$

Move to the output layer and calculate the output of each neuron:

$$y^s_{pk} = f(\sum_{j=1}^{L} w_{kj} \times y^c{}_{pj} \quad (7)$$

iii. Calculate the gradient of error starting with the gradient of error of the output layer and then the gradient of the hidden layer as shown in equations 8 and 9:

$$\partial_{pk} = (y^d_{pk} - y_{pk}) \times f'(\sum_{j=1}^{L} w_{kj} \times y^c{}_{pi}) \quad (8)$$

$$\partial_{pj} = f'(\sum_{i=1}^{N} w_{ji} \times x_{pi}) \times \sum_{k=1}^{M} w_{kj} \times \partial_{pk} \quad (9)$$

iv. Adjust the synaptic weights following equations 10 and 11:

$$w_{kj}(p+1) = w_{kj}(p) + \Delta w_{kj}(p) \quad (10)$$

$$w_{ji}(p+1) = w_{ji}(p) + \Delta w_{ji}(p) \quad (11)$$

v. Repeat the process for each example of the learning base until you reach a stop criterion (Tran, Bateni, Ki, & Vosoughifar, 2021).

4.1.3. Historical data and MLPNN architecture

The historical data of the temperature and wind speed data are obtained from MERRA-2 ("Global Modeling and Assimilation Office (GMAO) ", 2015). For the solar irradiation time series, the data is collected from the Copernicus Atmosphere Monitoring Service (CAMS) with a time step of 15 min ("Copernicus Atmosphere Monitoring Service CAMS, radiation service,"). After processing the meteorological data (organisation and screening out of scale values), 3 years data from March 02, 2013, to March 03, 2016 (3 years) are fed to the MLPNN which is characterized by 4 hidden layers, each one containing 10 neurons. The designed MLPNN requires 35,040 inputs in order to forecast the following 96 outputs. For example, to have a forecast of the meteorological data of April 04, 2020, data from April 03, 2017, to April 03, 2020, are considered as inputs. Table 2 shows the historical weather data used in this study, including input and output data size, data training and testing.

4.1.4. Forecasting strategy

The objective is to ensure a forecast of the meteorological data one day in advance using the collected historical data, named multi-inputs which train the MLPNN to have multi-outputs with several steps ahead (Abhishek *et al.*, 2012; Arcos-Aviles *et al.*, 2018; Tran *et al.*, 2021). Let x_t be meteorological data at time t, using actual and previously observed data. The multi-step ahead forecast estimates the future values of meteorological data from time (t + 1) up to (t + H) and can be expressed as the following (Mellit, Pavan, & Lughi, 2021):

$$\{\hat{x}_{t+1}, \hat{x}_{t+2}, \ldots, \hat{x}_{t+H}\} = f(x_t, x_{t-1}, \ldots, x_{t-k+1}) \quad (12)$$

Where: f is the forecast model used, H represents the forecast horizon, which is considered in our case as 96 time step in this article, k is the number of inputs which are the collected samples, $\{\hat{x}_{t+1}, \hat{x}_{t+2}, \ldots, \hat{x}_{t+H}\}$ is the output results of forecast model.

Table 2
Time series weather data forecast model.

Input features	Forecasting model	Input data size	Data training	Data testing	Output data size
Irradiance	MLPNN	3 years	From March 02,2013 To March 03,2016	From April 03, 2017 to April 03, 2020	24 hours ahead

Taking a case of 4 inputs (k=4), and horizon time step of 3 (H=3) the arrangement of the training matrix should be stated as follows:

$$\begin{vmatrix} x_5 & x_6 & x_7 \\ x_6 & x_7 & x_8 \\ x_7 & x_8 & x_9 \\ x_8 & x_9 & x_{10} \\ x_9 & x_{10} & x_{11} \\ . & . & . \\ . & . & . \\ . & . & . \end{vmatrix} = f \begin{vmatrix} x_1 & x_2 & x_3 & x_4 \\ x_2 & x_3 & x_4 & x_5 \\ x_3 & x_4 & x_5 & x_6 \\ x_4 & x_5 & x_6 & x_7 \\ x_5 & x_6 & x_7 & x_8 \\ . & . & . & . \\ . & . & . & . \\ . & . & . & . \end{vmatrix} \quad (13)$$

4.2. Optimization module

The best power planning in a set of possible solutions in the objective function given in equation (14), in which the fittest solution should be found using an optimization method. Consequently, an economic dispatch of energy flow is ensured and the energy imported from the main grid is reduced while maximizing the use of renewable energies (He *et al.*, 2019; Iqbal *et al*, 2018). Various optimization methods were proposed by scholars to solve the economic dispatch problem of microgrid system (Iqbal *et al*., 2018; Nimma *et al*., 2018; Zhai *et al.* , 2017). As long as the economical distribution of energy flows is a nonlinear problem and is a challenging task to solve, it is better to use artificial intelligence as an optimization tool (Faramarzi *et al* 2020). Many researchers extensively explore the performance of meta-heuristic algorithms and they have made comparative studies between these algorithms. In the next subsections the objective function, constraints and optimization method are presented and explained.

4.2.1. Objective function formulation

Covering the load demand efficiently using microgrid systems requires the optimization of its operating cost. For this aim, a number of issues should be simultaneously considered in the optimization. First, the fluctuation of PV and WT causes a mismatch between demand and supply. In addition, the purchase price of electricity from the power grid is higher during the peak load. As a result, the total operating cost of the system could be increased significantly. Therefore, it is necessary to apply a proper EMS based on a powerful algorithm that performs the energy dispatch, ensures the energy balance and reduces the operating costs (Iqbal *et al.,* 2018; Tayab *et al*., 2018; Wang *et al.*, 2017).

The main objective of our study is to minimize the operating cost of microgrid. The objective function can be described by equation (14) as follows (Wang *et al.*, 2017):

$$F = min \sum_{(t=1)}^{T} [(COST_{(PV,t)} + COST_{(WT,t)} + COST_{(grid,t)} + COST_{(BESS,t)}) \times T_{per} + COST_{(gen,t)}] \quad (14)$$

$$COST_{PV,t} = C_{PV} P_{PV,t} \quad (15)$$

Table 3
Operation and maintenance coefficient (Neto *et al.*, 2020).

Distributed sources	Operation and maintenance coefficient ($/kWh)
Photovoltaic generator (C_{PV})	0.00137
Wind turbine generator (C_{WT})	0.00646
Battery energy storage system (C_{BESS})	0.01

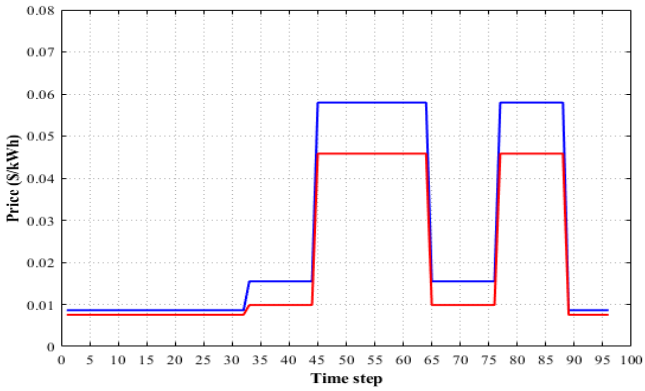

Fig 5. Main Grid electricity sale and purchase prices.

$$COST_{WT,t} = C_{WT} P_{WT,t} \quad (15)$$

$$COST_{grid,t} = C_{grid,t} P_{grid,t} \quad (16)$$

$$COST_{BESS,t} = C_{BESS} P_{BESS,t} \quad (17)$$

$$COST_{gen,t} = a + b \times P_{gen,t} + c \times P_{gen,t}^2 \quad (18)$$

T is the number of periods for a single day in which the 24 hours of the day are divided into 96 periods; each period will be 15 minutes long. $COST_{PV,t}$, $COST_{WT,t}$, $COST_{BESS,t}$ are the operating and maintenance cost of PV generator, WT generator, battery energy storage system respectively which are listed in Table 3. Eq.(19) is used to calculate the cost of power delivered from the diesel generator. Where a,b,c are the coefficients of the generator cost function: a=500 $/MWh, b=5.3 $/MWh, c=0 .004 $/MWh.

$COST_{grid,t}$ is the cost of electrical energy purchased or sold to the grid to cover the energy needs of the microgrid. $C_{grid,t}$ is the price of purchased power from the grid at a specific time, which varies according to Figure 6. The highest price is during the peak load period and it decreases during the low load period. The medium load period is characterized by an average price. The variation of sale and purchase prices from the power grid are illustrated in Figure 6.

4.2.2. Equality constraints

To ensure the reliability and proper operation of the system, it is necessary to assert the constraints of the energy balance such as the power balance, generators and battery limitations. It has been assumed that the power lines in the microgrid are relatively short compared to the distribution networks and the end-users. Hence, the wire losses are not taken into account in the calculation and modeling of microgrid. The balance constraint between load demand and production in the microgrid can be

expressed as follow by equation (20) (He *et al.*, 2019; Wang *et al.*, 2017):

$$P_{load,t} = P_{PV,t} \times \eta_{PV} + P_{WT,t} \times \eta_{WT} + P_{gen,t} + P_{grid,t} + P_{BESS,t} \quad (19)$$

Where: $P_{load,t}$, $P_{PV,t}$, $P_{WT,t}$, are the demand power, photovoltaic generator power, wind generator power forecasted a day-ahead at a time (t), respectively, $P_{gen,t}$, $P_{BESS,t}$, are the powers supplied by the generator and the battery energy storage system, $P_{grid,t}$ is the power generated by the grid.

4.2.3. Inequality constraints

The optimization of the objective function is implemented with respect to the constraints of the maximum and minimum power that can be supplied to the load from each source, which are defined in the following equations (T. Iqbal *et al.*, 2018; Wang *et al.,* 2017):

$$P_{grid,min} \leq Pgrid,t \leq P_{grid,max} \quad (20)$$

$$P_{gen,min} \leq Pgen,t \leq P_{gen,max} \quad (21)$$

$$P_{PV,min} \leq P_{PV,t} \leq P_{PV,max} \quad (22)$$

$$P_{WT,min} \leq P_{WT,t} \leq P_{WT,max} \quad (23)$$

BESS constraints can be presented in the following equations (He *et al.*, 2019; Wang *et al.*, 2017; Zhai *et al*, 2017):

$$P_{BESS,min} \leq P_{BESS,t} \leq P_{BESS,max} \quad (24)$$

$$E_{BESS,min} \leq E_{BESS,t} \leq E_{BESS,max} \quad (25)$$

The limits of the powers generated are listed in Table 4. The capacity of charge and discharge of the batteries for each period of time (15min) are limited as indicated in the equations (27) (28) (He *et al.*, 2019; Zhai *et al.,* 2017):

$$P_{dis,min} \leq P_{dis,t} \leq P_{dis,max} \quad (26)$$

$$P_{ch,min} \leq P_{ch,t} \leq P_{ch,max} \quad (27)$$

The BESS charge and discharge capacity limits of the microgrid studied are shown in Table 5:

Table 4
Limits of distributed generators and BESS

Type	Min Power (kW)	Max Power (kW)
PV	0	150
WT	0	80
Diesel gen	0	200
Grid	-50	150
BESS	18	90

Table 5
Charge and discharge BESS rate.

Operating modes	Min Power (kW)	Max Power (kW)
Discharge	0	10
Charge	0	-10

4.2.4. Marine predator algorithm

Marine predator algorithm is newly proposed algorithm for the optimization of single objective constrained engineering problem. This study proposes this method to solve the economic dispatch problem of the considered microgrid system.

4.2.5. Marine predator formulation

MPA algorithm is meta-heuristic method based on swarm intelligence. Over the search space, the first solution is uniformly distributed according to the following equation(Faramarzi *et al.*, 2020):

$$X_0 = Xmin + rand(X_{max} - Xmin) \quad (28)$$

Where X_{min} and X_{max} denote the lower and upper bounds for decision variables, and *rand* is a vector and their uniform, random values are in the range of 0 to 1.

An Elite matrix is constructed by the top predator which is considered as the fittest solution based on the survival of the fittest theory (the most talented in foraging predators). The arrays of this matrix play the role of searching and finding the optimal solution (prey) according to the prey's locations (Faramarzi *et al.*, 2020).

$$Elite = \begin{bmatrix} X^l_{1.1} & X^l_{1.2} & \cdots & X^l_{1.d} \\ X^l_{2.1} & X^l_{2.2} & \cdots & X^l_{2.d} \\ X^l_{3.1} & \vdots & \vdots & \vdots \\ \vdots & \vdots & \vdots & \vdots \\ \vdots & \vdots & \vdots & \vdots \\ \vdots & \vdots & \vdots & \vdots \\ X^l_{n.1} & X^l_{n.2} & \cdots & X^l_{n.d} \end{bmatrix}_{n\times d} \quad (29)$$

Where: X^l is the vector of the top predator, which is imitated n times to build up the Elite matrix. n denotes the number of predator's population (search agents), while d presents the dimension of decision variables(Eid *et al.,* 2021; Faramarzi *et al.*, 2020).

Since the prey is looking for their food, while the predators are searching for a prey, both predator and prey are assumed as search agents in this process. If another fittest predator at the end of each iteration replaces the top predator, the Elite matrix will be reconstructed. Based on another matrix called Prey with the same dimension as Elite, the predators change their locations based on it(Eid *et al.*, 2021). In other words, according to the fittest predator that constructs the Elite, the initialization process creates an initial Prey matrix which is presented by Eq 31(Faramarzi *et al.*, 2020):

$$\mathrm{Pr}ey = \begin{bmatrix} X_{1.1} & X_{1.2} & \cdots & X_{1.d} \\ X_{2.1} & X_{2.2} & \cdots & X_{2.2} \\ X_{3.1} & \vdots & \vdots & \vdots \\ \vdots & \vdots & \vdots & \vdots \\ \vdots & \vdots & \vdots & \vdots \\ \vdots & \vdots & \vdots & \vdots \\ X_{n.1} & X_{n.2} & \cdots & X_{n\times d} \end{bmatrix}_{n\times d} \quad (30)$$

Where, $X_{i,j}$ is the j th dimension of i th prey. It is worthy to mention that the optimization process is basically related to these two matrices.

4.2.6. MPA optimization scenarios

In order to simulate the different velocity ratio and entire life of a predator and prey, the optimization process of MPA can be separated into three main stages: (1) high velocity ratio, or the predator is moving slower than prey; (2) unit velocity ratio, or both predator and prey have almost the same pace; (3) low velocity ratio, or predator is moving rapidly than prey (Faramarzi *et al.*, 2020). These three groups include:

Stage 1: While mimicking the displacement of predators and prey, a precise iteration period is selected and allocated for each of the aforementioned phases, based on the nature laws that control prey and predator. The first phase occurs in early stages of the optimization, in which the exploration of search space has a great importance. Naturally, predator stops moving in high velocity ratio (v ≥10). This behavior is mathematically modeled as follows(Faramarzi *et al.*, 2020):

$$\begin{aligned} &While\ Iter < \frac{1}{3} Max\_iter \\ &\overrightarrow{stepsize_i} = \overrightarrow{R_B} \otimes \left(\overrightarrow{Elite_i} - \overrightarrow{R_B} \otimes \overrightarrow{\Pr ey_i} \right) \ i = 1, \ldots\ldots\ldots n \\ &\overrightarrow{\Pr ey_i} = \overrightarrow{\Pr ey_i} + P \times \overrightarrow{R_B} \otimes \overrightarrow{stepsize_i} \end{aligned} \quad (31)$$

In Eq (4), $\overrightarrow{R_B}$ presents a vector and their elements are random numbers based on Normal distribution representing the Brownian motion. The notation $\otimes$ indicates entry-wise multiplication. In the first third of iteration, prey is multiplied by R_B to simulate the prey movement for high exploration ability. Iter and Max_iter are current iteration and maximum one, respectively(Eid *et al.*, 2021; Faramarzi *et al.*, 2020). P is a constant number equals to 0.5, and R denotes a vector containing uniform random numbers in range [0,1].

Stage 2: In the second stage, both predator and prey are searching for their prey. In this intermediary phase, both the exploration and exploitation are of great importance in order to find an optimal solution. Therefore, half of population is devoted to exploration, where prey is responsible and second half of predator population is selected for exploration process. Naturally, if the prey displaces in Lévy, the best approach for predator is Brownian. While iteration number is between the first third and second third. For the first half of the population (Faramarzi *et al.*, 2020).

$$\begin{aligned} &\overrightarrow{stepsize_i} = \overrightarrow{R_L} \otimes \left(\overrightarrow{Elite_i} - \overrightarrow{R_L} \otimes \overrightarrow{\Pr ey_i} \right) \ i = 1, \ldots\ldots\ldots n/2 \\ &\overrightarrow{\Pr ey_i} = \overrightarrow{\Pr ey_i} + P \times CF \otimes \overrightarrow{stepsize_i} \end{aligned} \quad (32)$$

where $\overrightarrow{R_L}$ *presents* Lévy movement by a vector of random numbers based on Lévy distribution. Similarly, to the previous phase, the multiplication of R_L and prey mimics the behavior of prey in Lèvy. Since the Levy distribution has small steps size, this phase is improving the exploitation process (Faramarzi *et al.*, 2020).

$$\begin{aligned} &\overrightarrow{stepsize_i} = \overrightarrow{R_B} \otimes \left(\overrightarrow{Elite_i} - \overrightarrow{R_B} \otimes \overrightarrow{\Pr ey_i} \right) \ i = n/2, \ldots\ldots\ldots n \\ &\overrightarrow{\Pr ey_i} = \overrightarrow{\Pr ey_i} + P \times CF \otimes \overrightarrow{stepsize_i} \end{aligned} \quad (33)$$

CF is considered as adaptive factor in order to control the step size for predator movement while it equals

$$CF = \left(1 - \frac{Iter}{Max\_Iter} \right)^{\left(2\frac{Iter}{Max\_Iter} \right)}.$$

In the same line as the simulation of prey movement in second phase, the displacement of predator in Brownian behavior is simulated by the multiplication of $\overrightarrow{R_B}$ and Elite, while prey changes its location based on the displacement of predators in Brownian motion (Eid *et al.*, 2021; Faramarzi *et al.*, 2020; Sobhy *et al.*, 2021).

Stage 3: In the last stage, the high exploitation capability associates the optimization course. Consequently, the predator is Lévy in low velocity ration. This stage can be presented as follows(Faramarzi *et al.*, 2020; Sobhy *et al.*, 2021):

$$\begin{aligned} &While\ \ Iter > \frac{2}{3} Max\_iter \\ &\overrightarrow{stepsize_i} = \overrightarrow{R_L} \otimes \left(\overrightarrow{R_L} \otimes \overrightarrow{Elite_i} - \overrightarrow{\Pr ey_i} \right) \ i = 1, \ldots\ldots\ldots n \\ &\overrightarrow{\Pr ey_i} = \overrightarrow{Elite_i} + P \times CF \otimes \overrightarrow{stepsize_i} \end{aligned} \quad (34)$$

4.2.7. Eddy formation and FADs' effect

Inspired by the long jumps of sharks to find other environment with another possible prey, in case of as the eddy formation or Fish Aggregating Devices (FADs) effects, this behavior is mathematically modeled in order to avoid stagnation in local optima. The mathematical presentation of the FADs effect is as follows(Faramarzi *et al.*, 2020)

$$\overrightarrow{\Pr ey_i} = \begin{cases} \overrightarrow{\Pr ey_i} + CF\left[X_{\min} + \vec{R} \otimes \left(X_{\max} - X_{\min} \right) \right] \otimes \vec{U} & if\ r \le FADs \\ \overrightarrow{\Pr ey_i} + \left[FADs(1-r) + r \right] \left(\overrightarrow{\Pr ey_{r1}} - \overrightarrow{\Pr ey_{r2}} \right) & if\ r > FADs \end{cases} \quad (35)$$

Where FADs = 0.2 indicate the eventuality of FADs effect on the optimization process. $\vec{U}$ is the randomly binary vector with arrays including zero and one (Faramarzi *et al.*, 2020), its array is changed if it is less than 0.2 and one if it is greater than 0.2. r_1 and r_2 indicate random indexes of prey matrix, r is the uniform random number in [0,1].

4.2.8. Marine predator memory

According to the points highlighted, marine predators are distinguished by their good memory of reminding the location where they have been successful in foraging. A prey and FADs effect update is made to assess the ability of this matrix for fitness to update the Elite(Eid *et al.*, 2021). With each new iteration, the current fitness is compared to its equivalent in the previous iteration. If the current solution is more suitable, it replaces the previous solution. Following this iterative process, the quality of the

solution will be improved with the course of the iteration (Faramarzi *et al.*, 2020).

5. Results and discussions

Before proceeding with the optimization of operating cost, the forecast of temperature, irradiance and wind speed is carried out based on MLPNN. The results of root mean square error (RMSE), regression coefficient and mean absolute percentage error are listed in Table 6. It can be observed that the MLPNN has an acceptable RMSE, which ensures the prediction of temperature, irradiance and wind speed. Subsequently, it will be possible to have an approximate estimation of the microgrid system output power. Figure 7 depicts a comparison between the actual meteorological data and the forecasted values.

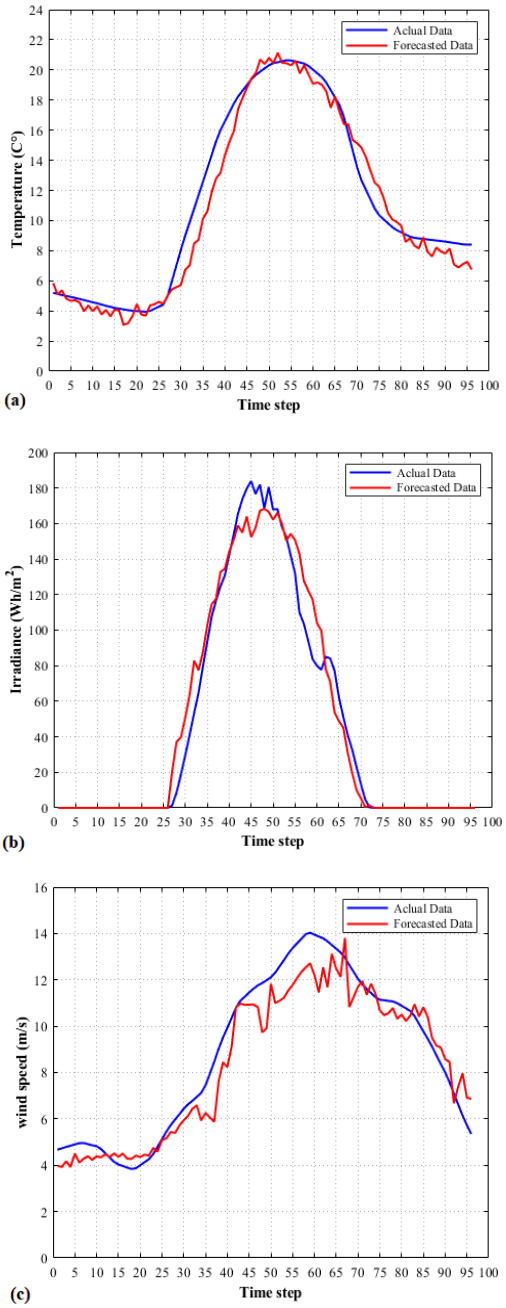

Fig 6. Actual and forecasted values: (a)temperature. (b)solar irradiance. (c) wind speed.

Table 6
Statistical errors for meteorological data.

Meteorological data	RMSE	Roh	MAPE
Temperature	1.45	0.979	0.105
Irradiance	25.00	0.914	0.323
Wind speed	0.73	0.953	0.049

Previously, the main grid covered the load of the commercial building, where its daily operating cost was around 229.051 $. In this work, we propose the integration of microgrid system to cover the load of this load as shown in Figure 1. Three scenarios are carried out in which different energy sources will be integrated in order to show the integration effect of the latter on the studied microgrid daily operating cost. Moreover, an optimization module based on MPA is applied to ensure an economic dispatch of microgrid energy flow.

Scenario 1: PV-Battery Energy Storage System, diesel Generator, and Distribution Grid (Only purchase)

The results of optimal economic dispatch for the first scenario are presented in Figure 8. It is found that the PV energy is completely used while it is available. The surplus PV power is stored in the BESS after satisfying the electricity demand. In order to minimize the consumption of electricity from the main grid, the diesel generator covers the electricity demand during peak hours when the price of electricity is high.

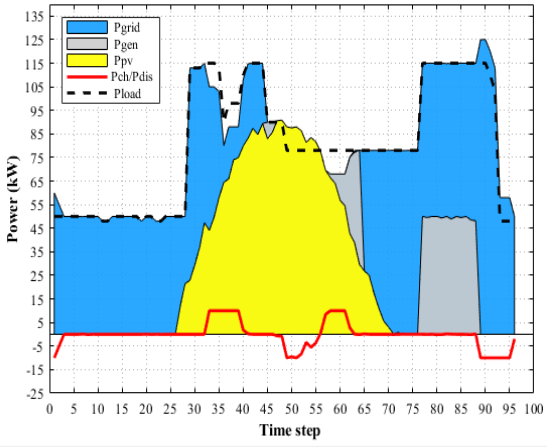

Fig 7. MPA based economic dispatch of powers of Microgrid (kW) by Scenario 1.

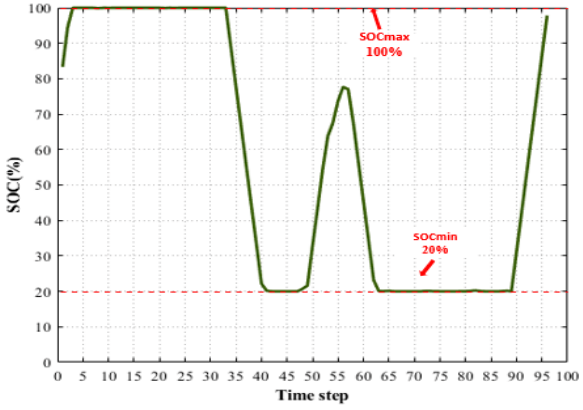

Fig. 8: State of charge of BESS for Scenario 1.

During peak hours, BESS could not cover the load since it has already reached its lower limit as shown in Figure 9. However, the BESS covers the load during the peak times of the day, and it is charged and billed by the main grid during low load periods which are characterized by the lowest purchase price of electricity.

The operation cost of this scenario is 150 $. A clear reduction of 34.51% is noted compared to that calculated before PV integration (Figure 16). This result confirms the expected contribution of PV energy and the BESS to the reduction of operating cost.

Scenario 2: PV, Wind, Battery Energy Storage System, diesel Generator and Distribution Grid (Energy purchase)

In the second scenario, a wind turbine has been added to the previous microgrid system. The daily operating cost is further decreased to 128.02 $. This implies a total reduction of 44.11% compared to the cost of main power grid as it is shown in Figure 17.

In this scenario, it is certain that the integration of an additional wind energy production contributes in the minimization of operating cost compared to scenario 1. Renewable energies cover the majority of load demand as Figure 15 illustrates.

Figure 10 represents the results of economic dispatch of energy flow of the microgrid studied by MPA for the second scenario. From Figure 10, during period 1 to 3, the BESS was charged from the main power grid. This can be explained by the low price of electricity and the SOC of the battery was not yet at its maximum allowable level. The surplus wind energy produced is used to charge the batteries while it does not reach its maximum charge level. In turn, BESS cover load during peak hours of the day in order to minimize purchasing power from the main grid.

The availability of wind power throughout the day led to a significant reduction of using power from the main power grid. Further, the diesel generator contributes in covering the electricity demand during the night when the purchase price from the main network is high. In addition, the BESS discharges during this peak hour until it reaches its minimum power (Figure 11).

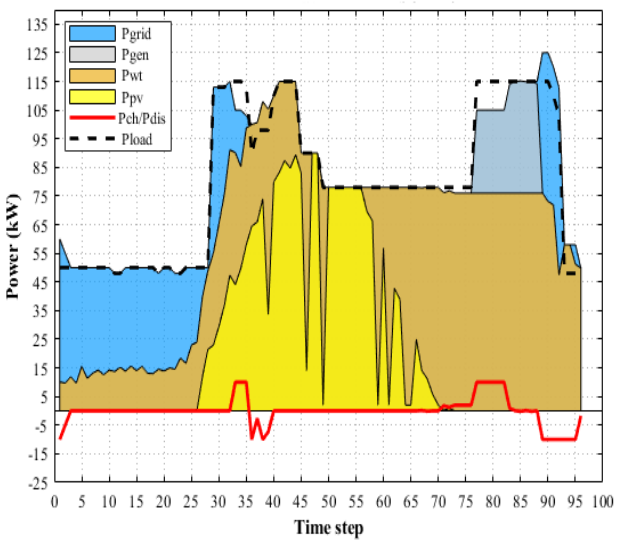

Fig 9. MPA based economic dispatch of powers produced by the Microgrid (Scenario 2).

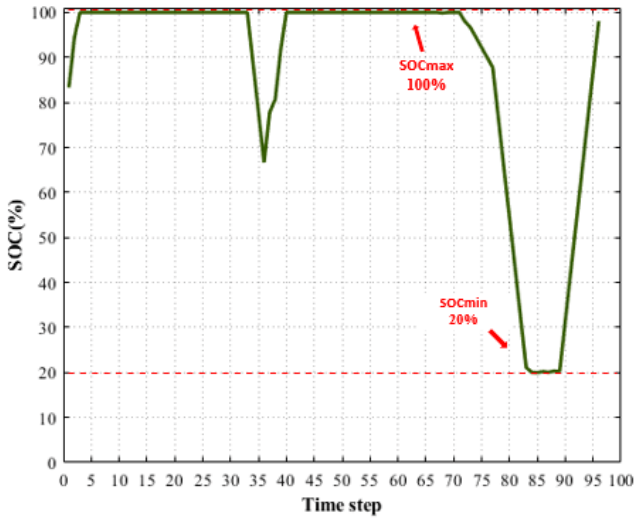

Fig 10. State of charge of BESS for Scenario 2.

Scenario 3: PV, Wind, Battery Energy Storage System, diesel Generator and Distribution Grid (purchase and sale of energy)

In the last scenario, it is possible to sell the surplus energy production from the two combined sources (photovoltaic and wind power plant) to the main grid. For this scenario, the results of the economic energy flow dispatch among all the generators in the microgrid are given in Figure 12. The majority of load has been covered by PV and wind energy as it is shown in Figure 15.

The total daily operating cost of the microgrid was 116.05 $, which implies a reduction of 49.33% (Figure 16) in comparison with that of the commercial building before transforming it to a microgrid, which is characterized by the integration of renewable energies and the possibility of buying and selling additional energy from the electricity grid.

Figure 13 illustrates the purchased/sold electricity from/to the main grid. The surplus wind power is sold to the main grid, which coincides with the high selling price of electricity. Consequently, the cost of the daily operation of the microgrid is remarkably decreased.

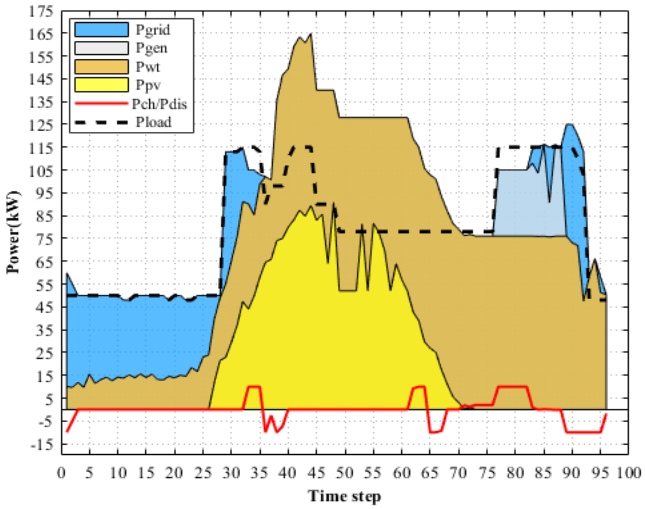

Fig 11. MPA based economic dispatch of powers of Microgrid (kW) by Scenario 3.

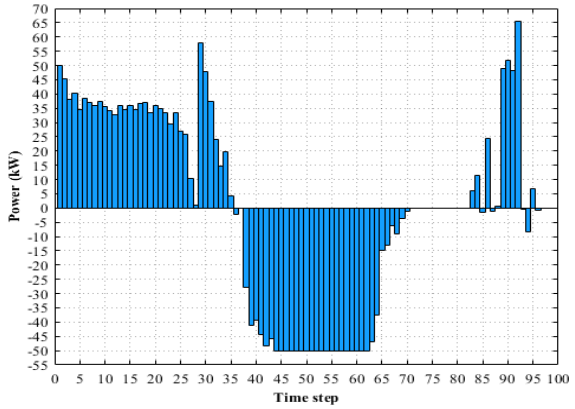

Fig 12. Sale and purchase of electricity from grid for Scenario 3.

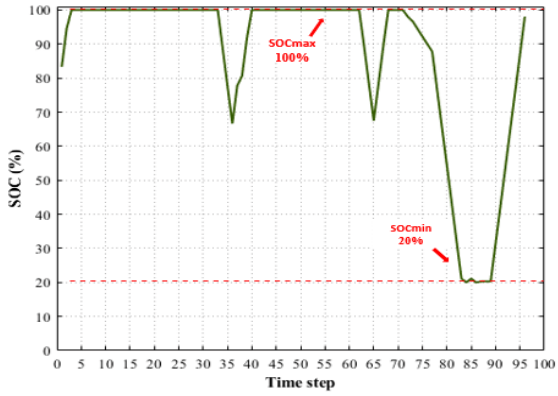

Fig 13. State of charge of BESS for Scenario 3.

From the period 85 to 93 (Figure12), the system bought the energy from the main grid even during the peak hours of the night because the renewable generators are not available. The battery energy storage system has reached its maximum energy level of 105 kWh during the first period of simulation. It is clear that MPA algorithm allowed charging and discharging of BESS economically while respecting the constraints of the battery. Moreover, the charging and discharging of the BESS do not exceed the limits shown in Table 4. The battery is charged by the additional wind energy produced and it is charged from the power grid during the night. The state of charge of BESS does not exceed the value of its maximum energy and the discharge is limited by its minimum energy (Figure 14).

Figure 15 depicts the share of each system in covering the electricity demand of the commercial building. In the first scenario, the power grid ensures more than 50% of the load. After integration of the wind system, the power grid share is reduced to 15%, and hence lower operating cost. In the second scenario, the wind power share is 51% of electricity demand due to the availability of wind speed in this area. In the last scenario, the renewable generators (PV-wind) cover more than 80% of the electricity demand, while less contribution of BESS is observed since the excess power has been sold to the grid.

In summary, Figure 16 depicts the operating cost of the studied microgrid configurations. In the first scenario, we optimize the economic dispatch of wind-PV system. Secondly, a wind turbine has been integrated to the microgrid system. The last scenario is distinguished by the possibility of selling excess energy from PV and wind to the main grid. Consequently, the daily operating cost is minimized by up to 49.33%. The contribution of both PV and wind energy plays a significant role in decreasing the operating costs and the integration of renewable energies as given in Figure 16.

6. Performance of MPA

This section analyses and compares both the MPA performance against the most used meta-heuristics gravimetric search algorithm (GSA), genetic algorithm (GA), optimization of the particle swarm (PSO). The analytical study shows that the marine predator algorithm converges rapidly to the minimum daily microgrid operating cost compared to other methods.

As Figure 17 and Table 7 show, there is a slight difference in daily operating cost obtained by the four meta-heuristic algorithms. Besides its ability to obtain a relatively lower operating cost, MPA has a rapid convergence towards the fittest solution in the earliest iteration (Figure 17).

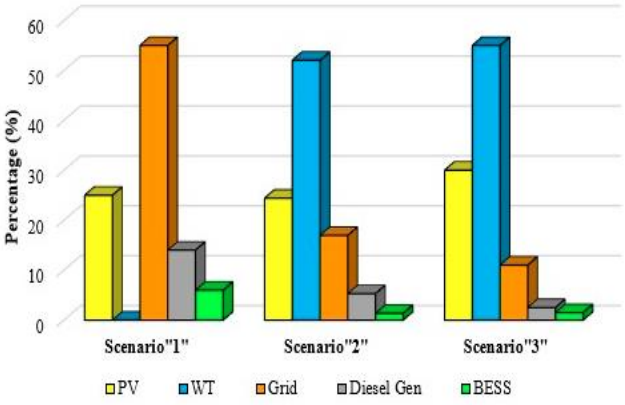

Fig 14. Daily sources share covering the load demand.

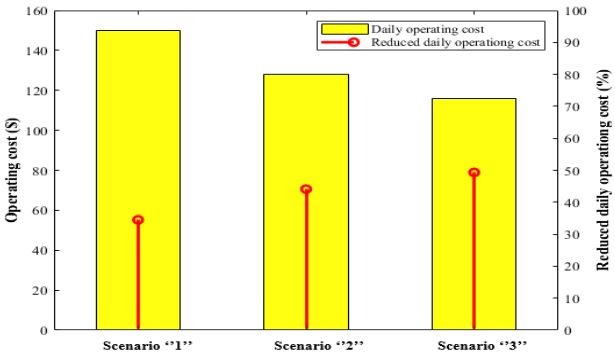

Fig 15. Daily operating cost of the microgrid and the percentage of its reduction for each scenario

Table 7
Daily microgrid operating cost of obtained by different meta-heuristic algorithms.

	MPA	PSO	GA	GSA
Daily operating cost ($)	**Scenario "1"**			
	150	150.44	150.79	129.25
	Scenario "2"			
	128.02	128.56	128.84	129.31
	Scenario "3"			
	116.05	116.6	116.87	117.23

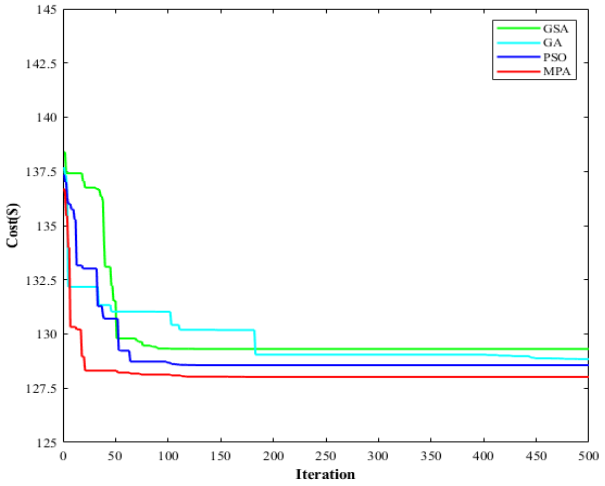

Fig 16. The convergence curves of MPA, PSO, GA, and GSA.

7. Conclusion

In this work, we have solved the economic dispatch problem for a microgrid system that covers the electricity demand of a commercial building in Algeria. For this aim, we proposed an energy management strategy based on MLPNN (forecast module) and MPA (optimization module). The weather data has been forecasted one day ahead and was validated using the regression and the root mean square error. After estimation of the output power of the microgrid, MPA ensures the optimal power flow while maintaining the least operation cost. In addition, different microgrid configurations under three scenarios are studied for the proposed EMS.

The first system configuration PV-BESS offered a 34.5% reduction in operating cost compared to the total price of electricity from the power grid. The costs were further minimized by 43.96% in the second scenario by adding a wind turbine to the previous system while it can only purchase power from the main grid. In the case of selling excess power to the main grid, the proposed EMS minimize daily operating cost by 49.33%. Thanks to the MPA and MLPNN that optimize the energy imported from the main network and increase the utilization of renewable energies. On one hand, purchasing energy from the main grid at peak times is avoided by making full use of integrated renewable energies. On the other hand, Time-of-Use pricing plays a key role in the final operating cost of the microgrid system. This was clear in the case of selling the excess production to the grid, where the operating cost was significantly reduced. The integration of renewable energy allows significant saving in operating costs, which contribute in recovering the high investment costs of installation in long-term benefits. Finally, it also preserves the environment and mitigates global warming.

References

Abhishek, K., Singh, M. P., Ghosh, S., & Anand, A. (2012). Weather Forecasting Model using Artificial Neural Network. *Procedia Technology*, 4, 311-318. doi:https://doi.org/10.1016/j.protcy.2012.05.047

Adrian Whiteman, S. R., Dennis Akande, Nazik Elhassan, Gerardo Escamilla and Iana Arkhipova, Renewable capacity statistics 2020 International Renewable Energy Agency (IRENA). 2020: Abu Dhabi. p. 66.

Al-Zoubi, H., Al-Khasawneh, Y., & Omar, W. (2021). Design and feasibility study of an on-grid photovoltaic system for green electrification of hotels: a case study of Cedars hotel in Jordan. *International Journal of Energy and Environmental Engineering*. doi:10.1007/s40095-021-00406-z

Arcos-Aviles, D., Pascual, J., Marroyo, L., Sanchis, P., & Guinjoan, F. (2018). Fuzzy Logic-Based Energy Management System Design for Residential Grid-Connected Microgrids. *IEEE Transactions on Smart Grid,* 9(2), 530-543. doi:10.1109/TSG.2016.2555245

Beccali, M., Cellura, M., Lo Brano, V., & Marvuglia, A. (2004). Forecasting daily urban electric load profiles using artificial neural networks. *Energy Conversion and Management*, 45(18), 2879-2900. doi:https://doi.org/10.1016/j.enconman.2004.01.006

Bochenek, B., Jurasz, J., Jaczewski, A., Stachura, G., Sekuła, P., Strzyżewski, T., . . . Figurski, M. (2021). Day-Ahead Wind Power Forecasting in Poland Based on Numerical Weather Prediction. *Energies*, 14(8). doi:10.3390/en14082164

Brenna, M., Corradi, A., Foiadelli, F., Longo, M., & Yaici, W. (2020). Numerical simulation analysis of the impact of photovoltaic systems and energy storage technologies on centralised generation: a case study for Australia. *International Journal of Energy and Environmental Engineering*, 11(1), 9-31. doi:10.1007/s40095-019-00330-3

Canales, F. A., Jurasz, J. K., Guezgouz, M., & Beluco, A. (2021). Cost-reliability analysis of hybrid pumped-battery storage for solar and wind energy integration in an island community. *Sustainable Energy Technologies and Assessments,* 44, 101062. doi:https://doi.org/10.1016/j.seta.2021.101062

Clarke, D. P., Al-Abdeli, Y. M., & Kothapalli, G. (2013). The impact of renewable energy intermittency on the operational characteristics of a stand-alone hydrogen generation system with on-site water production. *International Journal of Hydrogen Energy,* 38(28), 12253-12265. doi:https://doi.org/10.1016/j.ijhydene.2013.07.031

Copernicus Atmosphere Monitoring Service CAMS, radiation service. Retrieved from http://atmosphere.copernicus.eu/.

Crow, M., Gamage, T. T., Liu, Y., Nguyen, T. A., Qiu, X ., McMillin, B. M. (2015). A novel flow invariants-based approach to microgrid management. *IEEE Trans. Smart Grid*, 6(2), 516-525. doi: 10.1109/TSG.2014.2375064

Dahmoun, M. E.-H., Bekkouche, B., Sudhakar, K., Guezgouz, M., Chenafi, A., & Chaouch, A. (2021). Performance evaluation and analysis of grid-tied large scale PV plant in Algeria. *Energy for Sustainable Development*, 61, 181-195. doi:https://doi.org/10.1016/j.esd.2021.02.004

Dong, X., Li, X., & Cheng, S. (2020). Energy Management Optimization of Microgrid Cluster Based on Multi-Agent-System and Hierarchical Stackelberg Game Theory. *IEEE Access,* 8, 206183-206197. doi:10.1109/ACCESS.2020.3037676

Eid, A., Kamel, S., & Abualigah, L. (2021). Marine predators algorithm for optimal allocation of active and reactive power resources in distribution networks. *Neural Computing and Applications,* 33(21), 14327-14355. doi:10.1007/s00521-021-06078-4

Faramarzi, A., Heidarinejad, M., Mirjalili, S., & Gandomi, A. H. (2020). Marine Predators Algorithm: A nature-inspired metaheuristic. *Expert Systems with Applications*, 152, 113377. doi:https://doi.org/10.1016/j.eswa.2020.113377

Global Modeling and Assimilation Office (GMAO) (2015). Retrieved from http://www.soda-pro.com/web-services/meteo-data/merra

Guezgouz, M., Jurasz, J., & Bekkouche, B. (2019). Techno-Economic and Environmental Analysis of a Hybrid PV-WT-PSH/BB Standalone System Supplying Various Loads. *Energies*, 12(3). doi:10.3390/en12030514

Guezgouz, M., Jurasz, J., Bekkouche, B., Ma, T., Javed, M. S., & Kies, A. (2019). Optimal hybrid pumped hydro-battery storage scheme for off-grid renewable energy systems. *Energy Conversion and Management*, 199, 112046. doi:https://doi.org/10.1016/j.enconman.2019.112046

Guezgouz, M., Jurasz, J., Chouai, M., Bloomfield, H., & Bekkouche, B. (2021). Assessment of solar and wind energy complementarity in Algeria. *Energy Conversion and Management,* 238, 114170. doi:https://doi.org/10.1016/j.enconman.2021.114170

Hajer, M. A., & Pelzer, P. (2018). 2050—An Energetic Odyssey: Understanding 'Techniques of Futuring' in the transition towards renewable energy. *Energy Research & Social Science*, 44, 222-231. doi:https://doi.org/10.1016/j.erss.2018.01.013

He, L., Wei, Z., Yan, H., Xv, K., Zhao, M., & Cheng, S. (2019, 6-9 Sept. 2019). A Day-ahead Scheduling Optimization Model of Multi-Microgrid Considering Interactive Power Control. Paper presented at the 2019 4th International Conference on Intelligent Green Building and Smart Grid (IGBSG).

Iqbal, T., Khitab, Z., Girbau, F., & Sumper, A. (2018). Energy Management System for Optimal Operatioin of Microgrids Network. Paper presented at the 2018 IEEE International Conference on Smart Energy Grid Engineering (SEGE).

Iqbal, Z., Javaid, N., Iqbal, S., Aslam, S., Khan, Z. A., Abdul, W., . . . Alamri, A. (2018). A Domestic Microgrid with Optimized Home Energy Management System. *Energies*, 11(4). doi:10.3390/en11041002

Jurasz, J., & Ciapała, B. (2017). Integrating photovoltaics into energy systems by using a run-off-river power plant with pondage to smooth energy exchange with the power gird. *Applied Energy*, 198, 21-35. doi:https://doi.org/10.1016/j.apenergy.2017.04.042

Kaabeche, A., Diaf, S., & Ibtiouen, R. (2017). Firefly-inspired algorithm for optimal sizing of renewable hybrid system considering reliability criteria. *Solar Energy*, 155, 727-738. doi:https://doi.org/10.1016/j.solener.2017.06.070

Karthik, N., Parvathy, A. K., Arul, R., & Padmanathan, K. (2021). Multi-objective optimal power flow using a new heuristic optimization algorithm with the incorporation of renewable energy sources. *International Journal of Energy and Environmental Engineering*. doi:10.1007/s40095-021-00397-x

Kilickaplan, A., Dmitrii, B ., Onur, P., Upeksha, C., Arman, A., Christian, B. (2017). An energy transition pathway for Turkey to achieve 100% renewable energy powered electricity, desalination and non-energetic industrial gas demand sectors by 2050. *Solar Energy*, 158, 218-235.

Liu, H., Yu, C., Yu, C., Chen, C., & Wu, H. (2020). A novel axle temperature forecasting method based on decomposition, reinforcement learning optimization and neural network. *Advanced Engineering Informatics*, 44, 101089. doi:https://doi.org/10.1016/j.aei.2020.101089

Luu Ngoc, A., & Tran, Q.-T. (2015, 26-30 July 2015). Optimal energy management for grid connected microgrid by using dynamic programming method. Paper presented at the 2015 IEEE Power & Energy Society General Meeting.

Mellit, A., Pavan, A. M., & Lughi, V. (2021). Deep learning neural networks for short-term photovoltaic power forecasting. *Renewable Energy,* 172, 276-288. doi:https://doi.org/10.1016/j.renene.2021.02.166

Moran, B. (2016). Microgrid load management and control strategies. Paper presented at the 2016 IEEE/PES Transmission and Distribution Conference and Exposition (T&D).

Nezhad, M.M, Heydari, A., Groppi, D., Cumo, F., & Astiaso Garcia, D. (2020). Wind source potential assessment using Sentinel 1 satellite and a new forecasting model based on machine learning: A case study Sardinia islands. *Renewable Energy*, 155, 212-224. doi:https://doi.org/10.1016/j.renene.2020.03.148

Naeem, A., & Hassan, N. U. (2020, 7-9 March 2020). Renewable Energy Intermittency Mitigation in Microgrids: State-of-the-Art and Future Prospects. Paper presented at the 2020 4th International Conference on Green Energy and Applications (ICGEA).

Neto, P. J. d. S., Barros, T. A. d. S., Silveira, J. P. C., Filho, E. R., Vasquez, J. C., & Guerrero, J. M. (2020). Power Management Strategy Based on Virtual Inertia for DC Microgrids. *IEEE Transactions on Power Electronics*, 35(11), 12472-12485. doi:10.1109/TPEL.2020.2986283

Nimma, K. S., Al-Falahi, M. D. A., Nguyen, H. D ., Jayasinghe, S. D. G., Mahmoud, T. S., & Negnevitsky, M. (2018). Grey Wolf Optimization-Based Optimum Energy-Management and Battery-Sizing Method for Grid-Connected Microgrids. *Energies*, 11(4). doi:10.3390/en11040847

Peng, J., Fan, B., & Liu, W. (2021). Voltage-Based Distributed Optimal Control for Generation Cost Minimization and Bounded Bus Voltage Regulation in DC Microgrids. *IEEE Transactions on Smart Grid*, 12(1), 106-116. doi:10.1109/TSG.2020.3013303

Shaheen, M. A. M., Yousri, D., Fathy, A., Hasanien, H. M., Alkuhayli, A., & Muyeen, S. M. (2020). A Novel Application of Improved Marine Predators Algorithm and Particle Swarm Optimization for Solving the ORPD Problem. *Energies*, 13(21). doi:10.3390/en13215679

Sobhy, M. A., Abdelaziz, A. Y., Hasanien, H. M., & Ezzat, M. (2021). Marine predators algorithm for load frequency control of modern interconnected power systems including renewable energy sources and energy storage units. *Ain Shams Engineering Journal*. doi:https://doi.org/10.1016/j.asej.2021.04.031

Sonelgaz. Available online: http://www.sonelgaz.dz/ [accessed on 2020, A.

Stambouli, A. B., Khiat, Z., Flazi, S., & Kitamura, Y. (2012). A review on the renewable energy development in Algeria: Current perspective, energy scenario and sustainability issues. *Renewable and Sustainable Energy Reviews*, 16(7), 4445-4460. doi:https://doi.org/10.1016/j.rser.2012.04.031

Suberu, M.Y., Mustafa, M.W., & Bashir, N. (2014). Energy storage systems for renewable energy power sector integration and mitigation of intermittency. *Renewable and Sustainable Energy Reviews,* 35, 499-514. doi:https://doi.org/10.1016/j.rser.2014.04.009

Tang, X., Deng, W., & Qi, Z. (2014). Investigation of the Dynamic Stability of Microgrid. *IEEE Transactions on Power Systems*, 29(2), 698-706. doi:10.1109/TPWRS.2013.2285585

Tayab, U. B., Yang, F., El-Hendawi, M., & Lu, J. (2018, 7-8 Dec. 2018). Energy Management System for a Grid-Connected Microgrid with Photovoltaic and Battery Energy Storage System. Paper presented at the 2018 Australian & New Zealand Control Conference (ANZCC).

Theocharides, S., Venizelou, V., Makrides, G., & Georghiou, G. E. (2018, 10-15 June 2018). Day-ahead Forecasting of Solar Power Output from Photovoltaic Systems Utilising Gradient Boosting Machines. Paper presented at the 2018 IEEE 7th World Conference on Photovoltaic Energy Conversion (WCPEC) (A Joint Conference of 45th IEEE PVSC, 28th PVSEC & 34th EU PVSEC).

Ton, D. T., & Smith, M. A. (2012). The U.S. Department of Energy's Microgrid Initiative. *The Electricity Journal*, 25(8), 84-94. doi:https://doi.org/10.1016/j.tej.2012.09.013

Tran, T. T., Bateni, S. M., Ki, S. J., & Vosoughifar, H. (2021). A Review of Neural Networks for Air Temperature Forecasting. *Water,* 13(9). doi:10.3390/w13091294

Vergara, P. P., Torquato, R., & Silva, L. C. P. d. (2015). Towards a real-time Energy Management System for a Microgrid using a multi-objective genetic algorithm. Paper presented at the 2015 IEEE Power & Energy Society General Meeting.

Wang, S., Su, L., & Zhang, J. (2017). MPI based PSO algorithm for the optimization problem in micro-grid energy management system. Paper presented at the 2017 Chinese Automation Congress (CAC).

Zhai, M., Yajie, L., Tao, Z; Yan,Z . (2017). Robust model predictive control for energy management of isolated microgrids. in 2017 IEEE International Conference on Industrial Engineering and Engineering Management (IEEM).

Zhai, M., Liu, Y., Zhang, T., & Zhang, Y. (2017). Robust model predictive control for energy management of isolated microgrids. Paper presented at the 2017 IEEE International Conference on Industrial Engineering and Engineering Management (IEEM).